Preliminary Experimental Study of the Thermal Stability and Chemical Reactivity of the Phosphate-Based Binder Used in Al_2O_3-Based Ceramic Foam Filters (CFFs)

Cathrine K. W. SOLEM, Robert FRITZSCH and Ragnhild E. AUNE

Norwegian University of Science and Technology (NTNU),
Department of Materials Science and Engineering, Trondheim, Norway

Communicating author: cksolem@stud.ntnu.no, (+ 47) 404 76 828

Filtration of liquid aluminium is widely used in the industry for the removal of inclusions, and Ceramic Foam Filters (CFFs) are often the filtration media of choice. It is known that PH_3 (phosphine) can be released from used phosphate bonded CFFs when in contact with water. Additionally, there is a need of an improved understanding of the thermal stability and the chemical reactivity of these types of filters, as there is limited information available in the public domain.

In the present preliminary study, three CFFs, *i.e.* Substrate 1-3, with varying $AlPO_4$ (aluminium phosphate) content were studied under controlled conditions. Samples of the substrates, as produced and in contact with 5N pure aluminium, were heat-treated in a vacuum induction furnace at 850 °C and 1300 °C, as well as thermally studied at 850 °C using a Differential Scanning Colorimeter connected to a Thermogravimetric Analyser (DSC-TG). All tests were performed under an inert atmosphere of argon (Ar). Mass changes of ~0.001 % were registered for the pure substrates, and 0.003-0.10 % when in contact with aluminium. In the latter case, diffusion of P (phosphorous) from the bulk of the substrate to the interface was established to have taken place. A colour change, from white to orange/brown, was also observed at the interface, which is a clear sign that a chemical reaction has taken place. As a result, the thermal stability of the substrates can be questioned under present conditions.

Keywords: Filtration, Aluminium, Aluminium phosphide, Phosphate bond, Ceramic Foam Filters, CFF, Thermal stability, Chemical reactivity, HSE.

I.   INTRODUCTION

Filtration has for centuries been used to separate solids from liquids, and during the late 1970s´and early 1980s´ Ceramic Foam Filters (CFFs) were introduced as a possible filter media[1, 2]. CFFs have since then developed to become one of the most efficient filtration mechanisms of liquid aluminium[3]. However, filtration of aluminium reveal challenged both in regard to Health, Safety and Environmental (HSE) aspects, as well as issues related to the metal yield and quality of the produced material. The developments in the area of refining technology have, however, managed to close the gap between the service qualities of the products manufactured and the customer's demands. Nevertheless, more work is needed in order to meet the safety and environmental standards of today.

The refractory materials used in most CFFs today consist of an abundant inert ceramic material, as well as additional chemicals such as a binder and an absorbent aluminium phyllosilicate clay. The binder glues the material together and creates a slurry at room temperature. The slurry is dried, and the filter green body is fired[4]. The CFFs used to filter aluminium are often made of Al_2O_3 (alumina) with an $AlPO_4$ (phosphate) based binder and a rheology modifying clay. It has in this regards been suggested that, under certain conditions when $AlPO_4$-bonded CFFs are exposed to liquid aluminium alloys at high temperatures, it may start to decompose and reactions that allows for the production of AlP (aluminium phosphide) can occur[5]. The danger of producing AlP is that further reaction with water/moisture may generate PH_3 (g) that is extremely toxic and hazardous[6, 7].

It has also been reported in literature that $Ca_3(PO_4)_2$ (calcium hydroxyapatite), known as bone ash in the aluminium industry and used to fill cracks and holes in the launder, may decompose when in contact with different aluminium

alloys at high temperature. It was suggested that certain alloying elements, *e.g.* Mg (magnesium), acts as catalysts for the decomposition and further production of metal phosphides[5, 8].

In regards to the thermal stability and chemical reactivity of new (unused) $AlPO_4$-bonded CFFs an initial investigation has been performed by the present authors[9] to evaluate the potential for generation of PH_3 when in contact with water at ambient temperature. It was concluded based on this study that unused $AlPO_4$-bonded CFFs are non-reactive and safe to handle.

To improve the understanding of the decomposition of $AlPO_4$-bonded binders, used in ceramic refractories, at higher temperature the present study will focus on the generation and possible diffusion of P from three different phosphate-based Al_2O_3 CFF substrates, *i.e.* with different content of P. The filter medias (substrates) will be tested under different environmental conditions, and also when in contact with pure Al. All tests will be performed under controlled conditions in laboratory scale following strict safety measures.

II.   THEORY

A. Filtration

As previously mentioned, filtration is an often-applied refining method for removal of solids from liquids. All filtration processes are complex processes strongly dependent on *e.g.* the quality and chemical composition of the metal being filtered, as well as the filtration velocity. Within the physical filtration there are two main filtration modes, *i.e.* cake mode filtration and deep bed filtration.

Cake mode filtration is based on collecting inclusions from the melt on top of the filter media, forming a cake at the inlet surface. Hence, the inclusions are hindered from entering the filter due to a larger inclusion size than the pore size of the filter inlet. The formed filter cake can also act as a fine filter itself, removing inclusions while simultaneously increasing the thickness of the filter cake. Thus, the cake of particles restricts the metal flow and increases the flow resistance. This causes a higher-pressure drop over the filter, which unfortunately is not controllable during a filtration process. The filter cake will change as the size and size distribution of the collected inclusions change. The cake can be incompressible, *i.e.* the voids are constant with time, or compressible, *i.e.* the solid particles deform during filtration[3, 10].

Deep bed filtration is based on capturing inclusions inside the filter medium. The filter medias used have therefore larger pore openings at the inlet than in the case of cake mode filtration, allowing the inclusions to pass into the filter[3]. Inclusions are then removed from the melt by different interception and gravity mechanisms. Deep bed filtration depends on; firstly, that the inclusions have to be transported to the filter wall, and secondly, that the inclusions have to be retained to the filter wall[11, 12].

B. Ceramic Foam Filters (CFFs)

CFFs are suitable for filtration of all common aluminium wrought and foundry alloys, as well as for pure aluminium. The filters are distinguished by their base material and binder, as well as by the density of pores measured in Pores Per Inch (PPI) or in grade, which represents the cell size. The most commonly used filters in industrial cast houses are grades 30, 40, 50, 65 and 80 PPI, and grades ranging from 10 to 80[13, 14]. Moreover, CFFs with open pores have a structure consisting of rounded polyhedral[15, 16] connected to each other that creates a maze of cavities linked by a web of ceramic matrix material, see Figure 1. The filter cell, window and strut have been marked in the figure, *i.e.* the cell with a black dashed circle, two windows with smaller red circles, and the struts, which is the walls connecting the windows, with a black arrow.

C. Thermal Stability

As previously mentioned, when $AlPO_4$-bonded filters are exposed to liquid aluminium alloys AlP can be produced, which is also the case during the decomposition of $Ca_3(PO_4)_2$ if present in the launder[5, 8]. Equation (1) below illustrates a possible reaction when an aluminium alloy containing Mg is filtered by an $AlPO_4$-bonded Al_2O_3-based CFF, and Equation (2) the decomposition of the $Ca_3(PO_4)_2$ by the same alloy[8].
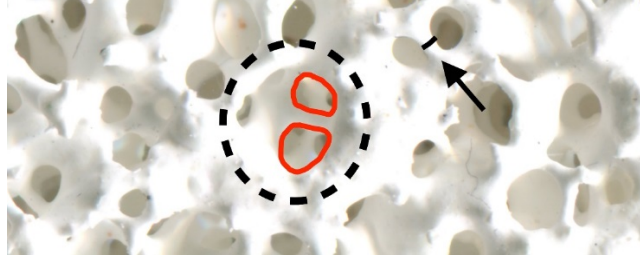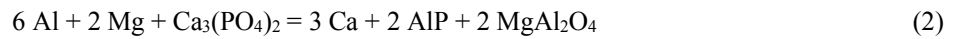
Figure 1: An open pore CFF with the cell, window and strut defined, i.e. the cell is marked with a black dashed circle, two windows with small red circles, and a strut with a black arrow.

$$2\ Al + AlPO_4 + Mg = AlP + MgAl_2O_4 \tag{1}$$

$$6\ Al + 2\ Mg + Ca_3(PO_4)_2 = 3\ Ca + 2\ AlP + 2\ MgAl_2O_4 \tag{2}$$

In Figure 2 the Gibbs free energy ($\Delta G°$) for reactions between 1 mole P and relevant aluminium alloying elements such as Al, Si, Fe, C, Ca and Na have been plotted. As can be seen in the figure, Fe and Ca have a higher affinity to P than Al, Si, C, and Na. The straight red line, seen in Figure 2 (a), represent the direct reaction of Al and P to form AlP, and it is above the two dotted lines that represent the reactions to form Fe_3P (green longer dashed line) and Ca_3P_2 (dark blue dashed line). This indicates that Fe_3P and Ca_3P_2 are more stable than AlP. From Figure 2 (b), it can also be seen that both Fe and Ca have a higher affinity to Al compared to P, and the reactions to form $FeAl_3$ and $CaAl_2$ will be favoured in comparison with Fe_3P and Ca_3P_2. As a result, AlP may be produced from the reaction between Al and P directly.
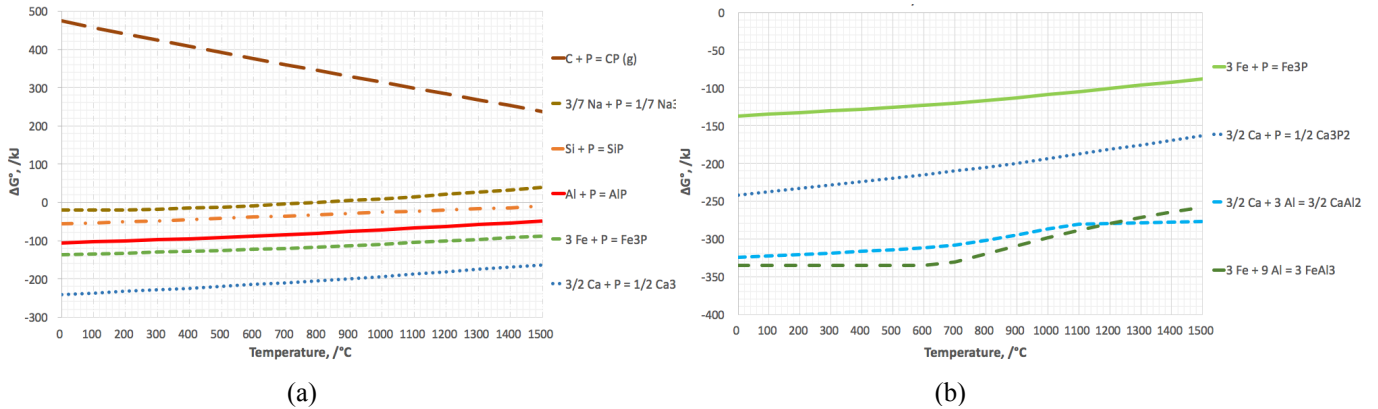

(a)

(b)

Figure 2: Gibbs free energies ($\Delta G°$) for different reactions in aluminium, where (a) shows elements reacting with 1 mole P to form metal phosphides, and (b) the affinity of Fe and Ca to Al and P, respectively.

III.   EXPERIMENTAL PROCEDURE

A. CFF Substrate Material

The materials investigated in the present study were three different CFF substrates, *i.e.* Substrate 1-3, see Figure 1. The substrates were all Al_2O_3-based, and the recipe used for the slurry was the same as the one used in the production of standard CFFs with varying amounts of P in the binder, *i.e.* Substrate 1 had the highest concentration of P and Substrate 3 the lowest.

B. Thermal Decomposition of the Binder during Heat Treatment

A vacuum induction furnace was used for heating the substrates, with and without additions of 5N pure aluminium, to test if any mass changes occurred. Firstly, the substrates were placed in carbon crucibles and heat-treated
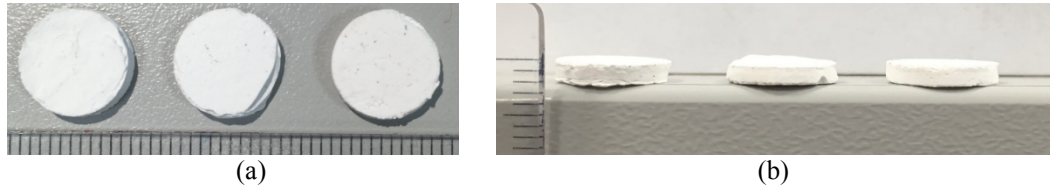
Figure 3: Diameter, (a), and height, (b), of CFF Substrates 1-3 (seen from the left). The bars are in mm, revealing diameters of 10.84 mm, 10.64 mm and 10.77 mm, and heights of 2.07 mm, 2.07 mm and 2.10 mm for Substrate 1-3, respectively.

individually at 1300 °C for 30 minutes, and at a later stage at 850 °C for 120 minutes, in an inert atmosphere of Ar (argon) with a purity of $\geq$ 99.999 %. Secondly, the substrates were placed in Al_2O_3 crucibles, covered with pieces of 5N pure aluminium and heat-treated for 120 minutes at 850 °C. A Differential Scanning Colorimeter connected to a Thermogravimetric Analyser (DSC-TG) was applied for further evaluation of the weight changes (NETZSCH model STA 449 C using a S-type thermocouple with a maximum temperature of 1600 °C). All experiments were performed under the same temperature intervals as presented in Table 1, and the experimental procedure was divided into the following three steps, *i.e.* (1) individual tests for each of the substrates, (2) tests with 5N pure aluminium, and (3) individual tests with the same substrate as in step (1) and the same amounts of metal as in step (2).

Table 1: The temperature intervals used during the DSC-TG analysis.

Initial temperature, /°C	End temperature, /°C	Heating rate, /°C/min	Holding time, /min
25	750	10	-
750	850	5	-
850	850	-	120
850	20	10	-

C. Microscopic Analysis

The substrates were examined using a Leica MeF4M light optical microscope (LOM) applying polarized green light (~550nm) to identify the presence of colour changes at the interface between the substrates and the molten aluminium, see Figure 4. The same samples were later evaluated with the use of the Electron Probe Micro Analysis (EPMA) technique.

During sample preparation, the substrates were first mounted in Epofix, and then cut by a diamond blade using water as the cooling media. The substrates were later sanded with the use of a 220P paper, and polished with 9 μm, 3μm and 1μm water-based diamond particles.
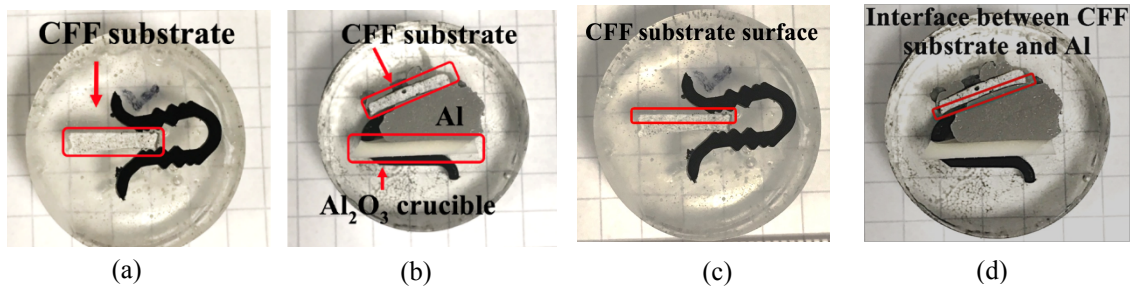

Figure 4: Images of the mounted substrates after heat-treatment where (a) is after step (1) and (b) after step (3). In (c) the surface of Substrate 2 is shown, and in (d) the interface between Substrate 2 and the 5N pure aluminium.

IV. RESULTS AND DISCUSSION

The weight changes recorded for the substrates, after heat treatment in the vacuum induction furnace at 1300 °C and 850°C respectively, are presented in Table 2. As can be seen from the table, significant weight losses were obtained

for all substrates with > 4 % for Substrate 1. It is, however, believed that the weight losses observed at 1300 °C were caused by sintering of the ceramic foam substrates and evaporation of the additives in the slurry. The experimental temperature was therefore lowered to 850 °C, and the changes in weight significantly reduced. The largest difference in weight was observed for Substrate 3 and measured to be ~0.14 %. The assumption that heating of the substrates above their sintering temperature had caused the major part of the weight loss recorded at 1300°C was strengthened.

Table 2: Recorded weight loss during heat treatment of Substrates 1-3.

Temperature, /°C	Substrate	m_0, /g	m, /g	Δm, /g	Δm, /%
	1	0.3366	0.3231	0.0135	4.0107
1300	2	0.2919	0.2819	0.0100	3.4258
	3	0.2920	0.2897	0.0023	0.7877
	1	0.3255	0.3253	0.0003	0.0921
850	2	0.3044	0.3043	0.0001	0.0329
	3	0.3548	0.3543	0.0005	0.1409

The experiments with the substrates in contact with 5N pure aluminium showed comparable results when heat-treated in the vacuum induction furnace, see Table 3. It was therefore decided to continue using 850 °C for the DSC-TG experiments, resulting in weight losses from 0.0727 % to 0.1 %.

Table 3: Weight changes for the heat-treated substrates in contact with 5N pure aluminium.

Experiment	Substrate X + Y Al	m_0, /g	m, /g	Δm, /g	Δm, /%
Vacuum induction furnace	1 + u g Al	14.8411	14.8415	0.00039	0.0026
	2 + v g Al	15.4233	15.4221	0.0012	0.0078
	3 + w g Al	14.0365	14.0352	0.0013	0.0088
DSC-TG	1 + x g Al	0.2238	0.2240	0.0002	0.0727
	2 + y g Al	0.2594	0.2597	0.0003	0.1010
	3 + z g Al	0.2759	0.2761	0.0002	0.0696

In Figure 5, the results from the DSC-TG experiments for step (3) is presented, *i.e.* (a) Substrate 1, (b) Substrate 2 and (c) Substrate 3, in contact with pure 5N aluminium. As can be seen from Figure 5 (a)-(c), the weight of each of the substrates is more or less stable during the heat treatment with only a minor increase in weight above ~ 600 °C in the case of Substrate 1 and ~ 400 °C in the case of Substrate 2 and 3 (blue straight lines, TG). It can also be seen from the heat flow curve (green striped lines) that there are two phase transformations occurring, *i.e.* one representing the melting of aluminium and the other the solidification.
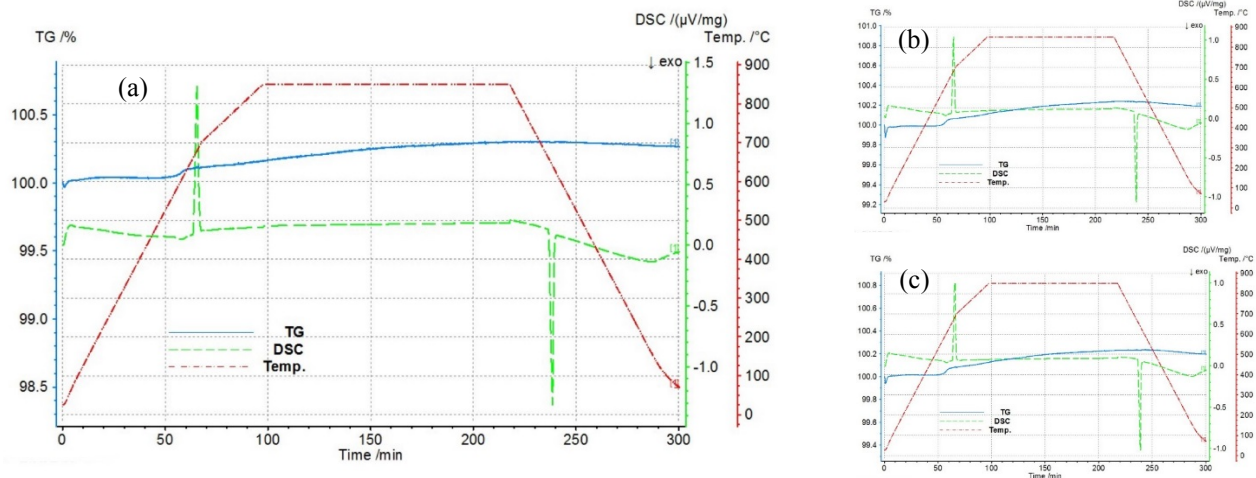

Figure 5: DSC-TG results for Substrate 1-3 presented in (a)-(c), respectively. The blue straight curve is weight (TG /%), the red stripe/dot is temperature (Temp. /°C), and the green striped is heat flow (DSC /µV/mg).

The melting temperatures for aluminium measured for Substrate 1-3 in the case of step (2) and step (3) are presented in Table 4. As can be seen from the table, most of the temperatures are close to the melting point of pure aluminium (660.5 °C), however, a significantly deviation can be seen for Substrate 3 when in contact with 5N pure aluminium (step (3)). This can only be explained by assuming that a chemical reaction has taken place shifting the melting temperature of the metal. It can also be seen from the figure that the enthalpy in the case of step (3) is significantly lower than for step (2). This is believed to be the result of Al and P reacting exothermically and releasing heat to the system.

Table 5: Melting temperatures and enthalpies for Substrate 1-3 based on the DSC-TG experiments.

Substrate	Step	Melting temperature, /°C	Enthalpy, /μV/mg
1	2	659.7	180.9
	3	657.7	122.2
2	2	657.9	165.9
	3	657.4	106.6
3	2	657.9	144.0
	3	683.8	104.8

All the substrates investigated in the vacuum induction furnace at 850 °C for 120 minutes, were further evaluated using LOM with polarized green light. In Figure 6 (a)-(c) images of Substrate 1-3 heat-treated at 850°C is presented. As can be seen from the images, no changes in the colour can be observed at the surface of the substrates. In Figure 6 (d)-(f) images of Substrate 1-3 heat-treated at 850 °C in contact with molten 5N pure aluminium is presented. In this case, however, a clear colour change from white to orange/brown can be seen in all images at the interface between the substrate and the metal. Moreover, it is seen that the thickness of the coloured boundary layer is thinnest in the case of Substrate 1 (~ 20 µm) containing the highest concentration of P, see Figure 6 (d). As the P content of the substrates decreases the thickness of the boundary layer increases, *i.e.* 80-100 µm for Substrate 2 and 240-340 µm for Substrate 3, Figure 6 (e) and (f) respectively.
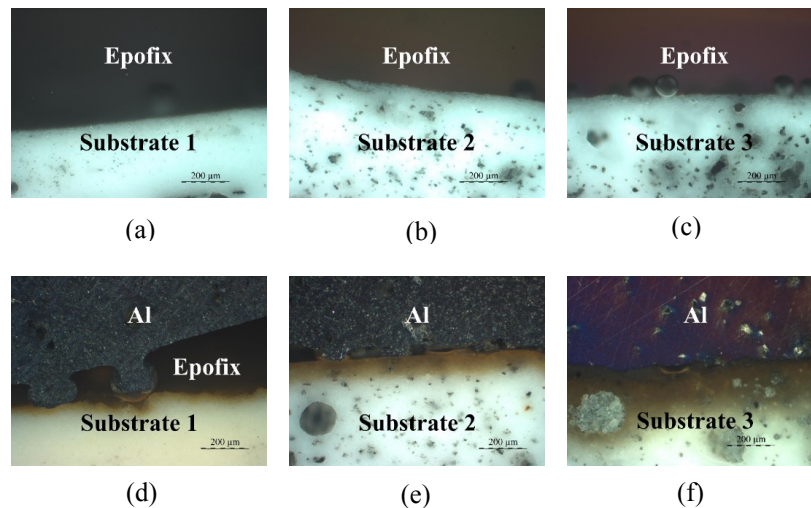

Figure 6: LOM images of heat-treated substrates taken with polarized light with 550 nm wavelength at 10X magnification. Images (a)-(c) are of Substrate 1-3, and images (d)-(f) of Substrate 1-3 in contact with 5N pure aluminium. The darkest orange/brown phase represent the reacted material.

The substrates shown in Figure 6 were further evaluated using EPMA. The results obtained for Substrate 3 (with the lowest concentration of P) are presented in Figure 7 (a)-(c). The surface of Substrate 3 in Figure 7 (a) and (b), as well as the interface between Substrate 3 and the 5N pure aluminium in Figure 7 (c), are all framed with a white dashed line representing the area of interest. As can be seen from Figure 7 (a), a slightly higher concentration of P is observed at the surface of the untreated substrate, *i.e.* within the framed area, compared to the P content of the rest of the matrix.
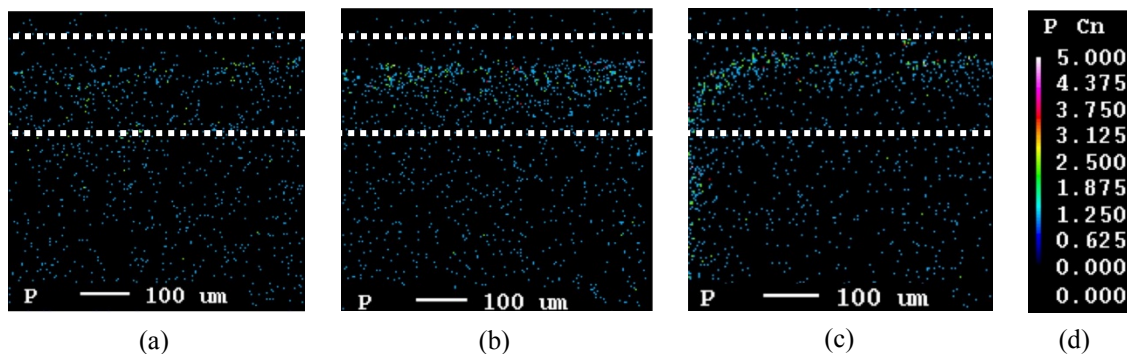
Figure 7: Electron Probe Micro Analysis (EPMA) images of Substrate 3, (a) as produced, (b) heat-treated, and (c) heat-treated in contact with 5N pure aluminium. The scale bar represented in (d) is valid for all images.

However, a homogeneous distribution of P in the bulk of the substrate can also be seen. For the heat-treated substrate represented in Figure 7 (b), a slight increase in the concentration of P at the surface can be seen, proving that P has diffused from the bulk to the surface. Quantitative data is, however, not available to determine the kinetic constant of this process. Finally, when Substrate 3 was put in contact with 5N pure aluminium, see Figure 7 (c), the concentration of P at the boundary layer between the substrate and the metal showed a similar trend. Based on the presently obtained results, it is believed that a gradual disintegration of the binder by diffusion of P out of the bulk into the boundary layer had taken place.

V.   CONCLUSION

For CFF Substrates 1-3, heat-treated in contact with 5N pure aluminium as well as without, it was concluded that diffusion of P had taken place from the bulk towards the surface/boundary layer of all the substrate materials. A clear colour change from white to orange/brown was also observed at the surface/boundary layer, as well as a quantitative concentration variation in regards to P at the interface between the substrate and the metal. The colour change indicates that a chemical reaction has taken place, and that the thermal stability of the substrates can be questioned under present conditions.

VI.   FUTURE WORK

The possibility of the production of AlP during heat treatment of CFF Substrates 1-3 will be further investigated by subjecting the substrates to different aluminium alloys, *i.e.* 3XXX, 5XXX and 6XXX, using the same experimental conditions as in the present study. Single alloying elements will be isolated to investigate if any catalytic effect exists. Even test in the presence of water/moisture will be conducted to evaluate the likelihood of generation of PH_3 (g).

ACKNOWLEDGEMENTS

REFERENCES

[1]   T. Sparks, Chapter 2 - History of Filtration, Solid-Liquid Filtration, Butterworth-Heinemann, Oxford, 2012, pp. 13-19.

[2]   C. Voigt, B. Fankhänel, E. Jäckel, C. Aneziris, M. Stelter, J. Hubálková, Effect of the Filter Surface Chemistry on the Filtration of Aluminum, Metallurgical and Materials Transactions B 46(2) (2015) 1066-1072.

[3]   S. Bao, Filtration of Aluminium-Experiments, Wetting, and Modelling, 2011.

[4]   J. Hejc, Private communication.

[5]   L. Aubrey, R. Olson, D. D. Smith, Development of a Phosphate-Free Reticulated Foam Filter Material for Aluminium Cast Houses, (2009).

[6]   Gas-Detect, Phosphine - PH3. https://www.gas-detect.com/gases-informations/ph3-gas-detector/.

[7]   F. Anger, F. Paysant, F. Brousse, I.L. Normand, P. Develay, Y. Galliard, A. Baert, M.A. Le Gueut, G. Pepin, J.-P. Anger, Fatal Aluminum Phosphide Poisoning, Journal of Analytical Toxicology 24(2) (2000) 90-92.
[8]   D.A. Doutre, Hazards associated with the use of bone ash in contact with molten aluminum, TMS Light Metals, 2010, pp. 797-800.
[9]   R. Fritzsch, Internal report from NTNU, 2017.
[10]   T. Engh, Principles of metal refining, Oxford University Press, Walton St, Oxford OX 2 6 DP, UK, 1992. 473 (1992).
[11]   S. Bao, M. Syvertsen, A. Kvithyld, T. Engh, Wetting behavior of aluminium and filtration with Al2O3 and SiC ceramic foam filters, Transactions of Nonferrous Metals Society of China 24(12) (2014) 3922-3928.
[12]   L.N.W. Damoah, L.F. Zhang, Removal of Inclusions from Aluminum Through Filtration, Metall. Mater. Trans. B-Proc. Metall. Mater. Proc. Sci. 41(4) (2010) 886-907.
[13]   Pyrotek®, Sivex Application Guidelines For Sivex Ceramic Foam Filtration Systems.
[14]   M.Smorawinski, J. Prebble , Private communication., 2017.
[15]   L.J. Gauckler, M.M. Waeber, C. Conti, M. Jacob-Duliere, Ceramic Foam For Molten metal Filtration, JOM 37(9) (1985) 47-50.
[16]   S.M. Ray, Brian; Keegan, Neil, Measurement of Filtration Performance, FIltration Theory and Practical Applications of Ceramic Foam Filters, 2005.